

# Measured Downlink Adjacent Satellite Interference of C-band satellites with 2° orbital separation

Wei-Chi IP, Chun-Yin VONG, *Member, IEEE*, and Rui ZHANG, *Member, IEEE*

**Abstract**— This paper presents a study of adjacent satellite interference (ASI) of two C-band (3400 – 4200MHz) commercial satellites AsiaSat 2 and AsiaSat 4, which are linear polarized, with 2° orbital separation in geostationary orbit (GEO). Series of measurements were performed to obtain the downlink ASI from AsiaSat 4 to the receiving antenna pointing to AsiaSat 2 satellite. Only the interference picked up by the antenna side lobe was considered in measurements by using large receiving antennas. Comparison between the theoretical analysis and measurements is given, verifying the results of the study theoretically and experimentally.

**Keywords**— Adjacent satellite interference, C-band, noise power, 2° orbital separation.

## I. INTRODUCTION

THE first true geostationary communication satellite, Syncom 3, was launched 48 years ago which marked a new epoch in aerospace [1]. Demand for satellite communication services has seen steady growth since then. Technical advances in communications and aerospace technologies are making satellites more powerful and functionally flexible. The number of GEO satellites increases rapidly as the market of satellite services exploded. There now exists more than 300 operational geostationary satellites [2]. Fig. 1 shows the actual number of C- and Ku-band operational satellites distributed in the GEO arc as of January 2010 [3].

Frequency spectrum is rare and valuable resource and only a limited portion is allocated for satellite communications. C-band (4/6 GHz) and Ku-band (12/14 GHz) are the most common frequency bands used in current commercial satellites. New and replacement GEO satellites are being launched and tend to be larger and more powerful. As a result, interference from adjacent satellites would become increasingly severe if not properly controlled. In the 1970's C-band satellites were separated by 5°, however international pressure to accommodate more geostationary satellites usage

This work has been funded and supported by Asia Satellite Telecommunications Company Limited (AsiaSat). All the measurements were done in the earth station of AsiaSat located in Hong Kong.

Wei-Chi IP is with the Asia Satellite Telecommunications Company Limited, Causeway Bay, Hong Kong (e-mail: [cip@asiasat.com](mailto:cip@asiasat.com)).

Chun-Yin Vong is with the Asia Satellite Telecommunications Company Limited, Causeway Bay, Hong Kong (e-mail: [fvong@asiasat.com](mailto:fvong@asiasat.com)).

Rui ZHANG is with the Asia Satellite Telecommunications Company Limited, Causeway Bay, Hong Kong (e-mail: [rzhang@asiasat.com](mailto:rzhang@asiasat.com)).

has gradually driven this separation down to 2.5. This small orbital separation, combined with the desire for smaller (low cost) antennas which take advantage of enhanced satellite performance places an increasing burden on the communications link which is in some cases dominated by adjacent satellite interference. It is a precious opportunity to measure the ASI among C-band satellites with 2° orbital separation as two satellites, operating in same frequency bands, co-coverage, co-polarization and owned by the same operator is very rare in the GEO arc.

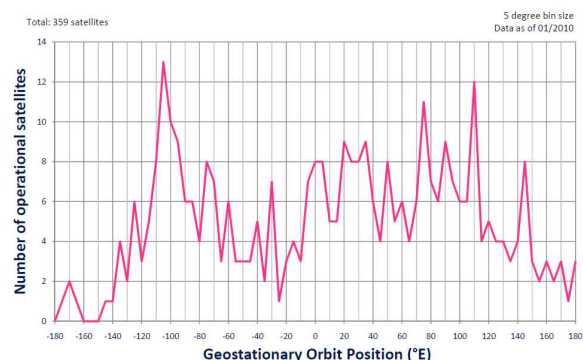


Fig. 1 The number of operational satellites distributed in the GEO arc

In this paper, measurement results of the downlink ASI of the two C-band satellites, AsiaSat 2 and AsiaSat 4 with 2° orbital separation are presented. Theoretical analysis based on a proposed mathematical model is given for comparison and verification.

## II. MATHEMATICAL MODEL AND THEORETICAL ANALYSIS

ASI is one of the critical issues in satellite communication networks. ASI can be broken down into two parts: uplink and downlink ASI. Both uplink and downlink ASI are transmitted or received via the antenna side lobes as illustrated in Fig. 2. For example, if the operation of the networks of satellite A and B is co-frequency, co-polarization and co-coverage, the antenna of receiving earth station Rx2 might receive uplink ASI from transmitting earth station Tx1 and downlink ASI from satellite A. The net effect of these ASI is the degradation of Bit-Error-Rate performance in digital satellite communications. In the paper, it mainly focused on the downlink ASI.

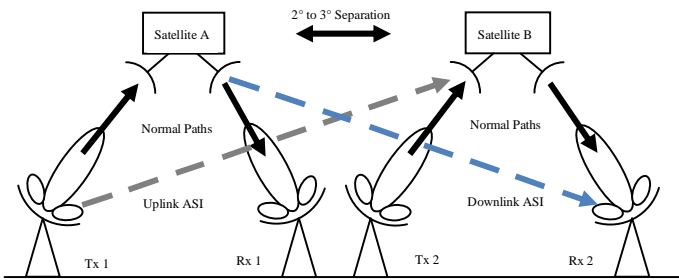


Fig. 2 Uplink and downlink ASI form an adjacent satellite network

To determine the downlink ASI, the most direct way is to measure the absolute value of ASI. However, this method is complex, time consuming and costly. Factors such as precise calibration of the downlink path for each channel (frequency dependent) and elimination of the sky noise are required to achieve an accurate result.

Therefore, instead of measuring the absolute value of ASI; using the sky noise as a reference to determine the ratio of  $ASI_{DL0} / N_{sky0}$  (at a particular frequency  $f_0$ ) makes the measurement easier and practical. Only common earth station equipment is needed and the variations of receiving path can be eliminated under the following conditions: Receiving signal strength is greater than the noise floor of spectrum analyzer in certain level (e.g. 8dB above) and noise temperature of LNA/LNB is not too high (e.g. below 30K for C-band).

The power density  $ASI_{DL0}$  of the downlink ASI (in Fig. 2) is given by [4]

$$ASI_{DL0} = \frac{EIRP}{4\pi R^2} \times G_R(\theta) \times \frac{\lambda^2}{4\pi} \times \frac{1}{BW} \quad (1)$$

where  $EIRP$  is the saturation EIRP of the satellite A transponder;  $\lambda$  is the wavelength in free space;  $R$  is the distance from satellite A to receiving earth station Rx2 which is location dependent;  $G_R(\theta)$  is the antenna off-axis gain of receiving earth station Rx2 at  $\theta$ ;  $BW$  is the interference noise bandwidth.

In (1), EIRP depends on the designed and manufactured characteristics of the satellite.  $G_R(\theta)$  is determined by the side lobe performance of the receiving antenna. Industrial practice is to envelope the antenna side lobe by (2) where  $\theta$  is the off-axis angle [5].

$$G(\theta) = 29 - 25 \log(\theta) \quad 1^{\circ} \leq \theta \leq 20^{\circ} \quad (2)$$

\* For antenna diameter  $D$  less than  $D/\lambda = 100$ , this value becomes  $100\lambda/D$  degrees.

The system noise temperature  $T_{sys}$  at the antenna flange [6] for an earth station can be computed by

$$T_{sys} = T_a + (l_l - 1) \times 290 + T_{re} \times l_l \quad (3)$$

where  $T_a$  is the antenna temperature in Kelvin, which depends

on frequency, antenna pattern and antenna elevation;  $l_l$  is the feed / waveguide loss; 290K is the assumed physical temperature of the waveguide; and  $T_{re}$  is the equivalent noise temperature of the receiving path (including the noise temperature of LNA/LNB, receiver and remaining RF/IF receiving system). In general,  $T_{re}$  can be approximated to the noise temperature of LNA/LNB which is the dominant contribution to  $T_{re}$  [6].

The downlink noise power density  $N_{DL0}$  [6] can then be calculated by

$$N_{DL0} = kT_{sys} \quad (4)$$

The importance of  $N_{DL0}$  is that this represents the minimum noise density level the earth station will receive. The clear sky noise power density  $N_{sky0}$  measured is the system noise of the antenna and almost equals to  $N_{DL0}$  when measuring the sky noise with a high elevation angle (e.g.  $70^{\circ}$  or above).

To investigate the contribution of downlink ASI power density to the sky noise power density, a simple mathematical model can be defined as

$$\text{Ratio} = \frac{\text{Downlink ASI Power Density}}{\text{Sky Noise Power Density}} = \frac{ASI_{DL0}}{N_{sky0}} \quad (5)$$

The clear sky noise  $N_{sky}$  received by the antenna and interference  $ASI_{DL}$  picked up by the antenna side lobe experience the same path gain/loss of the antenna receiving system as shown in Fig. 3.

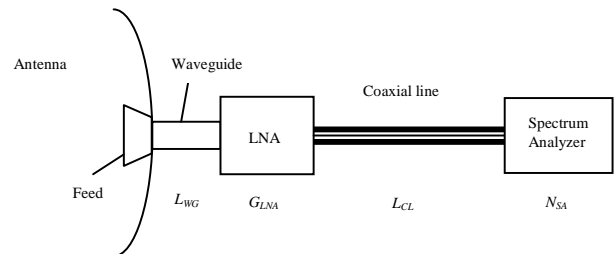


Fig. 3 Antenna receiving system

The power levels of sky noise and downlink interference measured by the spectrum analyzer are given as

$$N_{sky@SA}(f) = N_{sky}(f) \cdot L_{WG} \cdot G_{LNA} \cdot L_{CL} + N_{SA}(f) \quad (6)$$

$$ASI_{DL@SA}(f) = [ASI_{DL}(f) + N_{sky}(f)] \cdot L_{WG} \cdot G_{LNA} \cdot L_{CL} + N_{SA}(f) \quad (7)$$

where  $L_{WG}$  is the waveguide loss,  $G_{LNA}$  is the gain of LNA,  $L_{CL}$  is the cable loss,  $N_{SA}$  is the spectrum noise floor. Clear sky noise always exists and is one of the dominant noise sources received by antennas. Hence (5) can be calculated through the measurement.

$$\frac{ASI_{DL0}}{N_{sky0}} = \frac{ASI_{DL@SA}(f_0) - N_{sky@SA}(f_0)}{N_{sky@SA}(f_0) - N_{SA}(f_0)} \quad (8)$$

which is independent of the receiving path.

### III. MEASUREMENT CONSIDERATION

Radiation patterns of the receiving antenna consist of a number of side lobe and nulls. The actual angular receive position is important in this measurement. The downlink ASI was assumed to be picked up by the antenna side lobe. However, both peak level and angular position of side lobes and nulls in an antenna radiation pattern vary with frequency. Hence it is possible that the downlink ASI could be received at a null which would under-estimate the level of the downlink ASI for a particular antenna that may not fully represent real life network.

To assess the possibility of under-estimation, five antenna pointing positions with different azimuth and elevation were measured as shown in Fig. 4. If the power level measured at position 1 is lower than those at position 2, 3, 4 and 5, which means the downlink ASI was picked up by a null in the antenna pattern, the measurement would be discarded as a “bad measurement”. Since the antenna gain at the null in the antenna pattern is unpredictable, the result of the “bad measurement” is unreliable.

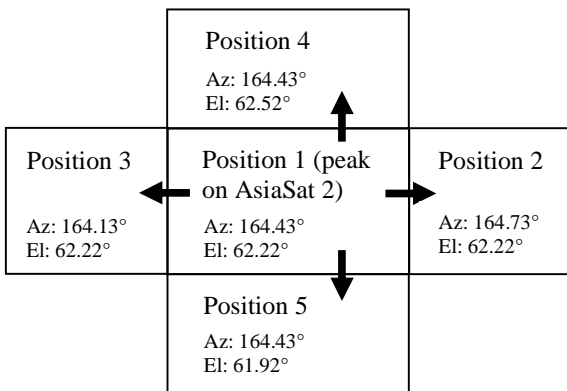


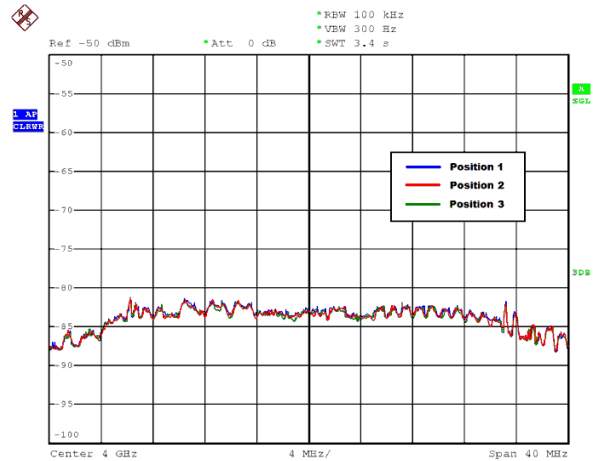
Fig. 4 Five antenna pointing positions with different azimuths and elevations

Fig. 5 shows measurement results of the five antenna pointing positions in a “good measurement”, i.e. the downlink ASI was not picked up by the null of the antenna side lobe. In Fig. 5 (b), the total receiving power over the whole channel is nearly constant even though the power levels of received signals at those three positions show a slight variation. Hence, it was considered as a “good measurement”.

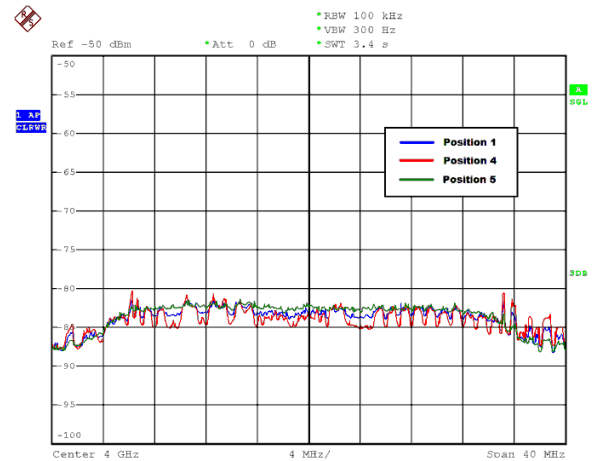
### IV. MEASUREMENT RESULTS AND DISCUSSIONS

Five 36 MHz C-band channels with different frequencies and linear polarizations (i.e. vertical and horizontal polarization) on AsiaSat 2 were measured. These five channels on the target satellite AsiaSat 2 were chosen because the

corresponding channels on the adjacent satellite AsiaSat 4 were operated in saturation mode. Thus, the effect of the downlink ASI to AsiaSat 2 would be the greatest. These channels on AsiaSat 2 were muted so that no signal except for the sky noise was picked up by the receiving antenna pointing to AsiaSat 2, i.e. no uplink ASI was received during the measurement.



(a)



(b)

Fig. 5 Five antenna pointing positions: (a) Azimuth changed with a constant elevation; (b) Elevation changed with a constant azimuth

Fig. 6 shows one plot of the measurement results recorded in a spectrum analyzer (SA). The plot consists of three lines demonstrating different power levels. The circled line presents the power level of  $ASI_{DL@SA}$ . Two flat lines present the SA noise  $N_{SA}$  and  $N_{sky@SA}$  respectively. Owing to the high directivity characteristic of earth station antenna,  $T_a$  is nearly constant when the antenna elevation angle is greater than 60° in C-band [7]. To measure the power level of the clear sky noise, the antenna should be at least pointed to a high elevation position (e.g. 10° - 15° above the normal elevation). At that position, contribution from other noise sources (e.g. ASI or ground noise etc.) shall be negligible because of high directivity characteristic of earth station antennas. The downlink ASI was measured by the antenna at an elevation

angle of 62.22° (normal elevation pointing to AsiaSat 2 at Hong Kong) and the sky noise was measured by the antenna at an elevation angle of 75.0°. Then the ratio of downlink ASI power density to the sky noise ( $ASI_{DLO} / N_{sky0}$ ) can be calculated by (8).

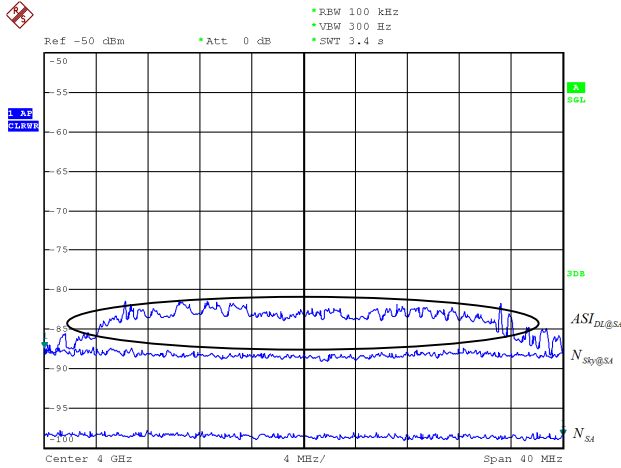


Fig. 6 Received noise and interference in a 36MHz C-band channel

Only ASI picked up by the antenna side lobe is considered in the measurement, hence the receiving antenna used would be limited by its size. A simple estimation of antenna pattern envelope is given by Recommendation ITU-R BO.1213 [8]. Fig. 7 shows the envelope of different antenna sizes.

Two antennas with a diameter of 6.3m and 4.5m respectively were used in the measurement to obtain downlink ASI power density at the particular orbital location (AsiaSat 2), where two adjacent satellites are only with 2° orbital separation. This is to ensure that ASI was not received via antenna main lobe.

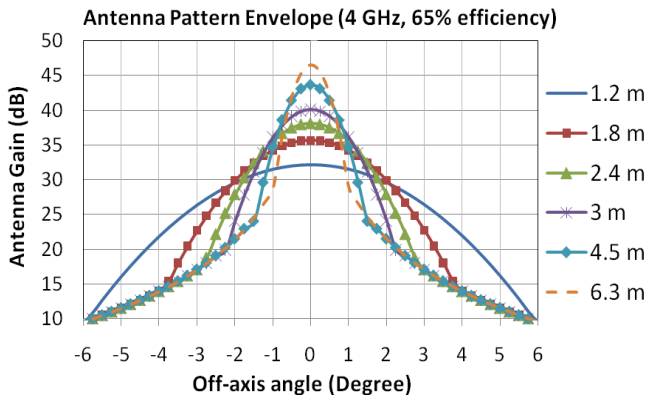


Fig. 7 Antenna pattern envelope of different antenna sizes

Table I shows the measurement results of the ratio of the downlink ASI power density to the sky noise in which the downlink ASI is from adjacent satellite AsiaSat 4 to the victim satellite AsiaSat 2.

The ratios of the downlink ASI power density to the sky

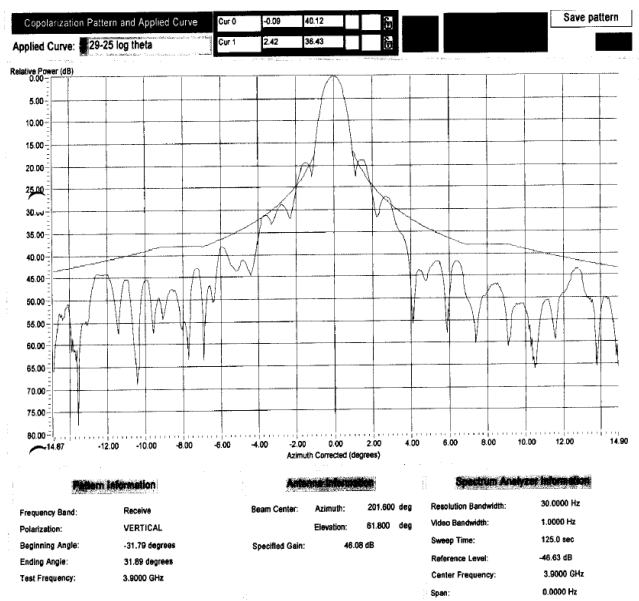
noise calculated by the proposed mathematical model are also given in Table I as a reference. In the computation, some assumptions were made: the antenna noise temperature is 45K; the feed / waveguide loss is 0.3 dB; the LNA / LNB noise temperature is 25K. The off-axis angle  $\theta$  used in the mathematical model is 2.3° instead of 2°. It is because the 2° orbital separation in geocentric coordinates equals to 2.3° of angular separation in topocentric coordinates in Hong Kong.

TABLE I  
DOWNLINK ASI TO SKY NOISE RATIO

Channel	Downlink Polarization	Receiving Antenna		Computation by mathematical model
		6.3m	4.5m	
1	vertical	1.0 dB	-2.8 dB	0.7 dB
2	vertical	1.0 dB	-4.9 dB	0.1 dB
3	vertical	4.4 dB	-1.4 dB	2.2 dB
4	horizontal	2.7 dB	-1.0 dB	0.7 dB
5	horizontal	4.2 dB	-1.3 dB	0.3 dB

As can be seen from the results, the power density of the downlink ASI received by the 6.3m antenna is about 5dB higher than that received by the 4.5m antenna in average. This phenomenon can be explained by Fig. 8 and 9, which are the radiation patterns of the 6.3m antenna (for both vertical and horizontal polarization) and the 4.5m antenna, respectively.

Only sky noise from the orbital location of AsiaSat 2 was received by the antenna main lobe as the corresponding channels on AsiaSat 2 were muted. All the downlink ASI was received by the antenna side lobe. It is seen from Fig. 8 that the measured radiation pattern of the 6.3m antenna exceeds the envelope of the antenna side lobe described in (2) at 2.3°, especially for horizontal polarization as shown in Fig. 8 (b), which is almost 3 to 4 dB higher than the envelope (i.e. delta is about -3 to -4 dB). For the 4.5m antenna, the side lobe performance is about 1 to 2 dB lower than the envelope (i.e. delta is about +1 to +2 dB). Correcting these deltas to the side lobe values, the interferences received by both antennas are consistent with the predicted ratio.



(a)

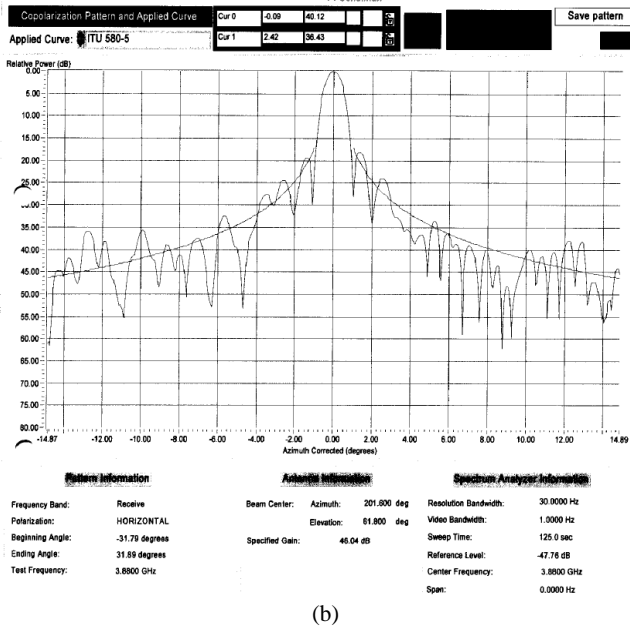


Fig. 8 The radiation pattern of the 6.3m antenna: (a) vertical polarization; (b) horizontal polarization

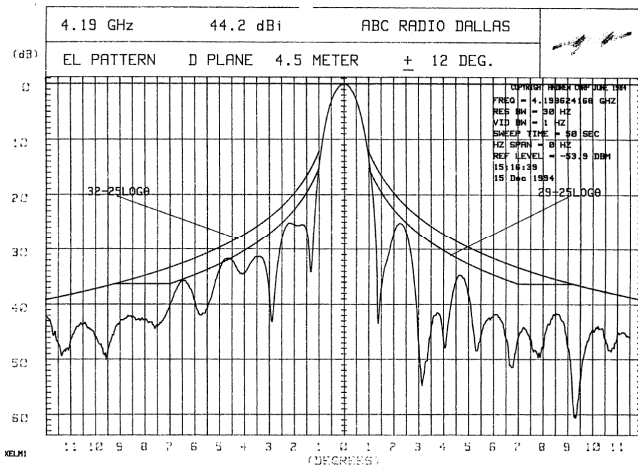


Fig. 9 The radiation pattern of the 4.5m antenna

V. CONCLUSION

Downlink ASI of two C-band satellites with 2° geocentric orbital separation was studied theoretically and experimentally. Two antennas of different sizes were used to investigate the effect of downlink ASI to the receive noise level of an earth station.

For receiving antennas whose side lobe profile is enveloped by the formula described in (2) and operated under the condition that the antenna main lobe is narrower than the orbital separation between satellites (i.e. 2° in this paper), the received downlink ASI from adjacent satellites will be independent of the antenna size. It can be further deduced from (1) and the included antenna patterns that earth station receiving noise level will be significantly affected by downlink ASI if downlink ASI is received by antenna main lobe.

This measurement did not take into account antenna variation, antenna installation (mis-pointing) and quality of antennas.

REFERENCES

- [1] R.J. Darcey (2012, May 14). Syncom 3 [Online]. Available: <http://nssdc.gsfc.nasa.gov/nmc/spacecraftDisplay.do?id=1964-047A>
- [2] Dr. T.S. Kelso. (2012, May 31). NORAD Two-Line Element Sets Current Data [Online]. Available: <http://www.celestrak.com/NORAD/elements/>
- [3] Mark C. J. Posen. "Have We Got a Slot," presented at the World Space Risk Forum 2010, Dubai, Mar. 2010.
- [4] R.E. Collin, *Antenna And Radiowave Propagation*. Int. ed., Singapore: McGraw-Hill, 1985, pp. 176-179; 206-207; 293-294.
- [5] *Radiation diagrams for use as design objectives for antennas of earth stations operating with geostationary satellites*, ITU-R RECOMMENDATION S.580-6, Jan. 2004.
- [6] Bruce R. Elbert, *The Satellite Communication Ground Segment and Earth Station Handbook*. Norwood, MA: Artech House, 2001, pp.176-181.
- [7] *Radio noise*, ITU-R RECOMMENDATION P.372-10, Oct. 2009.
- [8] *Reference receiving Earth station antenna pattern for the broadcasting-satellite service in the 11.7-12.75 GHz band*, ITU-R RECOMMENDATION BO.1213-1, Nov. 2005.